Title

Heparin-binding Properties of the Amyloidogenic Peptides Aβ and Amylin DEPENDENCE ON AGGREGATION STATE AND INHIBITION BY CONGO RED*

Journal

Journal of Biological Chemistry, 272(50)

ISSN

0021-9258

Authors

Watson, Deborah J

Lander, Arthur D

Selkoe, Dennis J

Publication Date

1997-12-01

DOI

10.1074/jbc.272.50.31617

THE JOURNAL OF BIOLOGICAL CHEMISTRY
Vol. 272, No. 50, Issue of December 12, pp. 31617–31624, 1997

Printed in U.S.A.

Heparin-binding Properties of the Amyloidogenic Peptides Aβ and Amylin

DEPENDENCE ON AGGREGATION STATE AND INHIBITION BY CONGO RED*

(Received for publication, July 10, 1997, and in revised form, September 10, 1997)

Deborah J. Watson‡, Arthur D. Lander§, and Dennis J. Selkoe‡¶

From the ‡Department of Neurology and Program in Neuroscience, Harvard Medical School, and Center for Neurologic Diseases, Brigham and Women's Hospital, Boston, Massachusetts 02115 and the §Department of Developmental and Cell Biology and Developmental Biology Center, University of California, Irvine, California 92697

Aggregation and deposition of the 40–42-residue amyloid β-protein (Aβ) are early and necessary neuropathological events in Alzheimer's disease. An understanding of the molecular interactions that trigger these events is important for therapeutic strategies aimed at blocking Aβ plaque formation at the earliest stages. Heparan sulfate proteoglycans may play a fundamental role since they are invariably associated with Aβ and other amyloid deposits at all stages. However, the nature of the Aβ-heparan sulfate proteoglycan binding has been difficult to elucidate because of the strong tendency of Aβ to self-aggregate. Affinity co-electrophoresis can measure the binding of proteoglycans or glycosaminoglycans to proteins without altering the physical state of the protein during the assay. We used affinity co-electrophoresis to study the interaction between Aβ and the glycosaminoglycan heparin and found that the aggregation state of Aβ governs its heparin-binding properties: heparin binds to fibrillar but not nonfibrillar Aβ. The amyloid binding dye, Congo red, inhibited the interaction in a specific and dose-dependent manner. The "Dutch" mutant $A\beta_{E22Q}$ peptide formed fibrils more readily than wild type Aβ and it also attained a heparin-binding state more readily, but, once formed, mutant and wild type fibrils bound heparin with similar affinities. The heparin-binding ability of aggregated $A\beta_{E22Q}$ was reversible with incubation in a solvent that promotes α-helical conformation, further suggesting that conformation of the peptide is important. Studies with another human amyloidogenic protein, amylin, suggested that its heparin-binding properties were also dependent on aggregation state. These results demonstrate the dependence of the Aβ-heparin interaction on the conformation and aggregation state of Aβ rather than primary sequence alone, and suggest methods of interfering with this association.

A hallmark of both Alzheimer's disease (AD)[1] and Down's syndrome is the presence of numerous extracellular deposits of the amyloid β-protein (Aβ), termed senile or neuritic plaques, in the brain parenchyma. In most cases, Aβ is also deposited in the walls of parenchymal and meningeal blood vessels. In these two types of deposits, Aβ exists largely in a fibrillar form consisting of 40 or 42 amino acid monomers aggregated into insoluble filamentous polymers. Aβ, which is derived by endoproteolysis from the β-amyloid precursor protein (1, 2), is by far the major constituent of plaques (3–5). However, several other plaque-associated proteins have been described, including α_1-antichymotrypsin (6), apolipoprotein E (7), the heparan sulfate proteoglycan (HSPG) perlecan (8), serum amyloid P component (9), and complement factors (10).

The order in which these various proteinaceous components are added to the senile plaques is not well understood, but some clues can be obtained from the composition of another type of Aβ deposit found in AD brains. "Diffuse" plaques are composed of Aβ in a particulate but not fibrillar form and do not react with the classic amyloid-staining dyes, Congo red and thioflavin S. Because the brains of young (<30 year old) Down's syndrome patients almost exclusively contain diffuse plaques, these deposits are believed to be the precursors of the compacted amyloid plaques, which invariably develop in older (>30–40 year old) Down's syndrome subjects (11, 12).

Snow and colleagues (8, 13) have detected immunohistochemically the presence of a specific HSPG, perlecan, in the compacted plaques and cerebrovascular amyloid of Alzheimer's disease brain. In addition, diffuse plaques in the hippocampus and cerebral cortex, but not in the cerebellum, were shown to contain perlecan (13, 14). Because compacted plaques are rarely found in the cerebellum even in end stage AD brains (15), it is postulated that HSPGs such as perlecan could play a role in the transition of diffuse Aβ deposits into compacted amyloid. The finding that cortical diffuse plaques in Down's syndrome brain are also perlecan-immunoreactive (13) is consistent with this hypothesis. HSPGs may play a general role in the formation and stabilization of many types of amyloid, since they have also been identified in association with amyloid deposits in virtually all other human amyloid diseases (for review, see Ref. 16).

In AD cerebrovasculature, Aβ amyloid deposits have been ultrastructurally localized to the vascular basement membrane region of capillaries, arterioles, and small arteries (17), where perlecan is a prominent constituent. In addition, one of the diseases linked genetically to β-amyloid precursor protein (He-

* This work was supported in part by a predoctoral fellowship from the Edward R. and Anne G. Lefler Center at Harvard Medical School (to D. J. W.), National Institutes of Health Grants AG 06173 and AG 12749 (to D. J. S.) and National Institutes of Health Grant NS 26862 (to A. D. L). The costs of publication of this article were defrayed in part by the payment of page charges. This article must therefore be hereby marked "*advertisement*" in accordance with 18 U.S.C. Section 1734 solely to indicate this fact.

¶ To whom correspondence should be addressed: Center for Neurologic Diseases, Brigham and Women's Hospital, Harvard Institutes of Medicine, 77 Ave. Louis Pasteur 740, Boston, MA 02115. Tel.: 617-525-5200; Fax: 617-525-5252.

[1] The abbreviations used are: AD, Alzheimer's disease; Aβ, amyloid β-peptide; HSPG, heparan sulfate proteoglycan; ACE, affinity co-electrophoresis; HCHWA-D, Hereditary Cerebral Hemorrhage with Amyloidosis, Dutch-type; HPLC, high performance liquid chromatography; CSF, cerebrospinal fluid; NaMOPSO, 3-[*N*-morpholino]-2-hydroxypropanesulfonic acid, sodium salt; LMW, low molecular weight; HFIP, (1,1,1,3,3,3)-hexafluoroisopropanol.

reditary Cerebral Hemorrhage with Amyloidosis, Dutch-type (HCHWA-D)) causes a particularly severe deposition of Aβ in meningocerebral blood vessels (18, 19), again suggesting an important role for a vascular basement membrane factor in Aβ deposition.

Previous attempts to characterize the binding between HSPGs and Aβ (20–23) have been hindered by the unique difficulties of working with synthetic Aβ, a highly hydrophobic 40–42-amino acid peptide that readily precipitates into insoluble aggregates *in vitro*. Affinity co-electrophoresis (ACE) is an advantageous method to characterize the binding of proteins to proteoglycans or their glycosaminoglycan side chains (24, 25). Each component is freely mobile within a highly porous native agarose gel, and no coupling of either component to any matrix, resin, or solid support is required, so all of the potential binding surfaces remain available. Importantly, Aβ has less opportunity to aggregate during the experiment than in many other types of binding assays.

In this paper, we use ACE to characterize the binding of Aβ peptides to heparin (a glycosaminoglycan that is frequently used as a model for tissue heparan sulfates) at physiological pH and ionic strength. Both wild type Aβ and the HCHWA-D disease-causing mutant form were studied. We show that the heparin-Aβ interaction is critically dependent on the secondary structure and aggregation state of Aβ and is potently inhibited by the amyloid-binding dye Congo red. Aβ containing the HCHWA-D mutation binds heparin more readily than wild type peptide due to its increased tendency to form fibrils, not because of a greater affinity for heparin. Finally, we demonstrate that another amyloid-forming subunit, human amylin, also binds to heparin, whereas the nontoxic and non-amyloidogenic rat isoform of amylin does not.

EXPERIMENTAL PROCEDURES

Peptide Preparations and Electron Microscopy—Wild type $A\beta_{1-40}$ peptide was synthesized and HPLC-purified by Dr. D. Teplow (Biopolymer Laboratory, Brigham and Women's Hospital). $A\beta_{1-40}$ containing the E22Q "Dutch" mutation ($A\beta_{E22Q}$) was made by Dr. D. Chin (University of Missouri, Columbia) and aliquots were HPLC-purified by Dr. D. Walsh (Biopolymer Facility, Brigham and Women's Hospital). Human and rat amylin peptides were purchased from Peninsula Laboratories (Belmont, CA) or Bachem (Torrance, CA). The amino acid sequence of wild type human $A\beta_{1-40}$ is DAEFRHDSGYEVHHQKLVFFAEDVGSNKGAIIGLMVGGVV (see, *e.g.* Ref. 1); in mutant $A\beta_{E22Q}$, Glu^{22} (underlined) is changed to Gln (19).

For amylin and nonfibrillar Aβ preparations, lyophilized peptides were freshly resuspended in water (initially at 1 mM) and used immediately. Alternatively, fibrillar Aβ was formed by resuspending the lyophilized peptide in water to 1 mM, then adding artificial cerebrospinal fluid (CSF; 150 mM NaCl, 3 mM KCl, 1.7 mM $CaCl_2$, 0.9 mM $MgCl_2$ in 1.5 mM phosphate buffer, pH 6.5) to achieve a final concentration of 100 μM Aβ peptide and rocking it for 2 days at room temperature, followed by centrifugation at 16,000 × *g* for 15 min. The pellet was resuspended in ACE electrophoresis running buffer (50 mM NaMOPSO in 125 mM acetate buffer, pH 7.0; Ref. 24) and sonicated before use. A similar protocol using an ultrafiltrate of CSF showed $A\beta_{1-40}$ fibril formation after 48 h at room temperature (26).

Duplicate aliquots of each peptide preparation were collected and the peptide concentrations were determined by amino acid analysis, performed by M. Condron (Brigham and Women's Hospital Biopolymer Laboratory). Simultaneously, aliquots of each peptide preparation were applied to a 200-mesh copper-Formvar/carbon grid (EM Sciences, Gibbstown, NJ), negatively stained with 2% uranyl acetate, and observed with a JEOL JEM 100CX-II electron microscope at 60 kV. Congo red birefringence was determined by the protocol of Castaño *et al.* (27).

Heparin Tracer Preparation—Tyramine was added to the reducing ends of unbleached heparin molecules (Grade I, porcine intestinal mucosa, Sigma) via a reductive amidation reaction (28). This method adds ≤1 tyramine per heparin molecule and does not disturb the chemistry of the heparin along its chain length. The tyramine moiety was iodinated by the IODOGEN method (Pierce), and the heparin was then size-fractionated by gel filtration. The low molecular weight (LMW) fraction (≤ 6 kDa) was used to minimize the number of potential binding sites per heparin molecule. Unlabeled LMW-heparin was from Sigma.

Affinity Co-electrophoresis—Horizontal 1% (w/v) agarose gels were cast with two combs essentially as described (24, 25), producing a set of nine rectangular wells and a perpendicularly oriented slot (Fig. 1). Serial dilutions of each peptide preparation were prepared in ACE electrophoresis running buffer (see above) and mixed with an equal volume of molten 2% agarose, cast into the nine wells, and allowed to set. The slot was loaded with ^{125}I-LMW-heparin, which was subjected to electrophoresis through the protein-containing zones. After drying the gels, the positions of bands were measured using a PhosphorImager 400A and ImageQuant software (Molecular Dynamics). Staining the gels with Coomassie Brilliant Blue showed that Aβ itself did not noticeably migrate from its original position during the electrophoresis times used (not shown).

From positions of labeled bands, a retardation coefficient, R, was calculated ($R = (M_o - M)/M_o$, where M_o is the mobility of free heparin and M is heparin's observed mobility through a protein (*i.e.* Aβ)-containing zone; Ref. 24). Values were fit to the equation $R = R_\infty/(1 + (K_d/[\text{protein}])^n)$ (25). In general, better fits were obtained with $n = 2$, suggesting either positive cooperativity in binding, or perhaps the fact that some Aβ fibrils are lost on the walls of tubes and pipette tips in the process of making serial dilutions, causing Aβ concentrations to be somewhat overestimated at the highest dilutions. Protein concentrations are given in units of molarity of monomer, and were determined by amino acid analysis. Values for K_d were calculated using these units of molarity; a calculation based on the molarity of polymerized fibrils would yield a much lower K_d (see "Discussion").

Solution Phase Binding Assay—Preparations of fibrillar or nonfibrillar Aβ were incubated for 1 h at room temperature with ^{125}I-LMW-heparin in ACE electrophoresis buffer. In some cases, serial dilutions of Congo red or of unlabeled LMW-heparin were included; these solutions were made fresh for each experiment. The mixtures were then transferred to nitrocellulose by vacuum filtration through a dot-blot apparatus, followed by one rinse with phosphate-buffered saline. The filter was dried and the bound radioactivity retained on the filter was counted directly in a γ counter (Cobra II AutoGamma, Packard Instruments). Background radioactivity in control wells containing ^{125}I-LMW-heparin tracer alone were subtracted from the values for Aβ-containing wells before analysis. Values from six control wells containing only Aβ and heparin tracer were averaged to provide a value for maximum Aβ-heparin binding.

RESULTS

Fibrillar, but Not Non-fibrillar, Aβ Binds Heparin—ACE experiments to measure the binding of Aβ to heparin were initially attempted using aliquots of lyophilized wild type $A\beta_{1-40}$ that were freshly resuspended in water, diluted, and assayed immediately. Samples were incorporated into the nine lanes of a 1% agarose gel, and ^{125}I-LMW-heparin was subjected to electrophoresis through those lanes (Fig. 1*A*). At neutral pH, the mobility of Aβ is much less than that of heparin (data not shown), so we expected a complex of heparin and Aβ to have a mobility significantly less than that of free heparin. Assuming this is the case, any binding of Aβ to heparin should have been revealed as a series of electrophoretic bands that were progressively retarded with increasing Aβ concentration (Fig. 1*B*). In contrast, no effect of Aβ on heparin mobility was seen at peptide concentrations up to 243 μM (Fig. 2*A*).

These data indicate that either Aβ and heparin do not bind under the conditions of the assay, or that binding could not be detected because the mobility of the Aβ-heparin complex is not sufficiently different from that of heparin alone. To test the latter possibility, we reversed the roles of heparin and peptide in the experiment (25). In this case, heparin was cast into the nine parallel lanes, and ^{125}I-Aβ introduced into a single slot perpendicular to the lanes. Because heparin is more mobile than Aβ, the peptide-containing slot was placed between the heparin lanes and the anode (Fig. 1*C*). In this experiment, any binding of heparin to Aβ should have been revealed as a series of electrophoretic bands whose mobility was progressively increased by increasing heparin concentrations. However, as

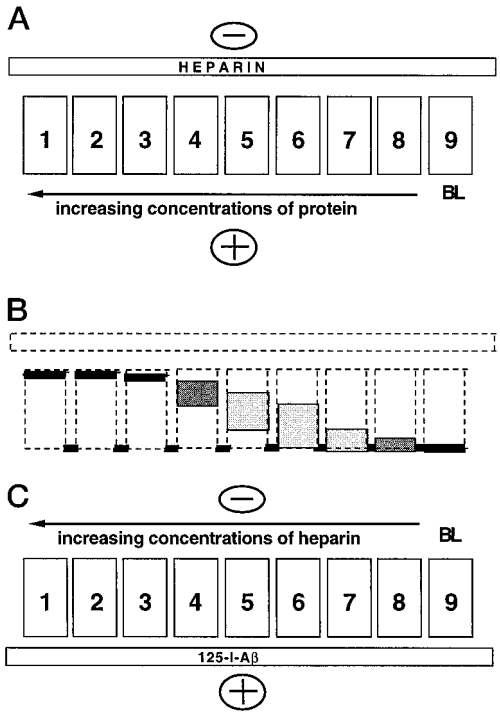

FIG. 1. **Method of affinity co-electrophoresis.** *A*, top view of lanes in a schematic horizontal agarose gel. ^{125}I-Heparin is loaded into the horizontal slot at the top of the gel. Varying concentrations of the potential heparin-binding protein of interest are loaded in vertical *lanes 1–8*, and *lane 9* serves as a buffer blank. The heparin is electrophoresed through the protein-containing wells toward the positive electrode. *B*, expected pattern of bands for a heparin-binding protein. *Lane 9* represents the mobility of unbound heparin. Increasing concentrations of protein shift the mobility of heparin toward the top of the protein lane. *C*, schematic diagram of reverse ACE. Radioiodinated protein (*i.e.* ^{125}I-Aβ) is loaded into a slot between the anode and nine parallel lanes containing increasing concentrations of unlabeled glycosaminoglycan (*i.e.* heparin).

shown in Fig. 2*B*, no change in the mobility of ^{125}I-Aβ was seen at heparin concentrations up to 10 mg/ml (>1.5 mM).

As before, the only way we could have failed to detect actual binding of heparin and Aβ in this experiment is if the mobility of the heparin-peptide complex was not significantly different from that of the labeled species, in this case Aβ. However, it is not possible for the mobility of the heparin-Aβ complex to be indistinguishable from both that of free Aβ and that of free heparin, as Aβ and heparin have mobilities that are very different from each other. Thus, the negative results in Fig. 2, *A* and *B*, together indicate that freshly resuspended Aβ and heparin do not bind each other ($K_d \geq 0.25$ mM).

Because the close association of heparan sulfate with Aβ deposits in AD brain still suggested an important interaction between the two molecules, we next considered the possibility that the secondary structure of polymerized fibrillar Aβ creates a heparin-binding epitope. To aggregate Aβ into fibrils, aliquots of lyophilized $A\beta_{1-40}$ were resuspended initially in water and then diluted into artificial CSF and rocked for 48 h at room temperature. Electron microscopy of the pelleted precipitate confirmed the formation of straight, unbranched filaments approximately 10 nm in diameter (Fig. 2*D*), similar to the structure and dimensions of Aβ fibrils purified from Alzheimer's plaques (29, 30). Furthermore, after staining with Congo red, Aβ fibrils showed birefringence under polarized light (not shown). In contrast, electron microscopy of the freshly resuspended nonfibrillar Aβ preparation demonstrated large amorphous clumps (Fig. 2*C*), indicating the presence of aggregated but not fibrillar Aβ. Upon reaction with Congo red, the nonfibrillar Aβ was not birefringent (not shown).

Increasing concentrations of the Aβ fibrils were then loaded into the lanes of an ACE gel and tested for heparin binding. In sharp contrast to what was observed with the freshly resuspended peptide, low micromolar concentrations of fibrillar Aβ completely retarded the mobility of the heparin tracer (Fig. 2*E*). To confirm that the retardation was due to a specific binding interaction and not to nonspecific physical blockage of the heparin by a dense network of fibrils, we demonstrated that the binding of ^{125}I-LMW-heparin to Aβ fibrils could be completely competed away by excess unlabeled LMW-heparin (Fig. 2*F*).

Several independently aggregated fibril preparations showed electrophoretic retardation profiles very similar to that shown in Fig. 2*E*. To measure binding affinity, we calculated retardation coefficients, R, from each of several ACE gels. The results from five experiments were fit to the equation $R = R_\infty/(1 + (K_d/[\text{protein}])^2)$ (25, 31), which yielded an average K_d of 1.31 ± 0.10 μM (Fig. 3; this value is expressed in units of molarity of Aβ monomer (see "Experimental Procedures")).

As an independent test of the results obtained by ACE, a solution-phase binding assay was also used. Increasing concentrations of fibrillar or nonfibrillar Aβ were incubated with ^{125}I-LMW-heparin in solution, after which the mixtures were applied to a nitrocellulose membrane by vacuum filtration and counted to measure the retained (protein-bound) heparin. Again, fibrillar but not non-fibrillar Aβ bound heparin with a low micromolar affinity (not shown).

Congo Red Blocks the Binding of Heparin to Aβ Fibrils—Congo red is a histochemical dye used for the detection of amyloids of all types in tissue sections. The binding of Congo red to Aβ has been postulated to depend in part on fibrillar Aβ structure (32). We tested whether Congo red could inhibit the binding of heparin to fibrillar Aβ. Equal aliquots of fibrillar $A\beta_{1-40}$ were incubated with increasing concentrations of Congo red, and then loaded into the lanes of an ACE gel. Compared with the control lanes of Congo red alone (Fig. 4*A*, *lane 7*) and fibrils alone (*lane 8*), a dose-dependent inhibition of heparin binding to the fibrils was observed (*lanes 1–6*).

We also used the solution-phase binding assay (above) to confirm the interaction of Congo red with fibrillar Aβ. In the ACE gels, an inhibition of heparin-protein binding is most readily visualized when the protein concentration in the lanes containing no inhibitor is high enough to completely retard the migration of heparin (see, *e.g.*, Fig. 4*A*, *lane 8*). However, using the solution-phase binding assay, we were able to test a range of Aβ concentrations to show that the IC_{50} for Congo red inhibition of heparin binding increases with increasing protein concentration (Fig. 4*B*). When similar concentrations of Aβ were compared in the two assays, ACE gels showed a higher IC_{50} for Congo red than the solution-phase assay (Fig. 4, *A versus B*, *middle trace*). This may be due to the migration of the negatively charged Congo red out of the well during ACE electrophoresis, decreasing the total amount of drug in the lane.

HCHWA-D Mutant Aβ Fibrils Have an Affinity for Heparin Similar to That of Wild Type Fibrils—HPLC-purified $A\beta_{1-40}$ containing the E22Q (HCHWA-D) substitution was either freshly resuspended from a lyophilized aliquot or aggregated into fibrils as described above. Serial dilutions of each preparation were loaded into the lanes of ACE gels and tested for binding to ^{125}I-LMW-heparin. The freshly resuspended peptide did not bind to heparin up to peptide concentrations of 15.2 μM (Fig. 5*A*, *lane 1*), whereas 5.7 μM fibrillar $A\beta_{E22Q}$ almost completely retarded the mobility of heparin (Fig. 5*B*, *lane 4*).

From autoradiograms of ACE gels such as that in Fig. 5*B* retardation coefficients were calculated and plotted against

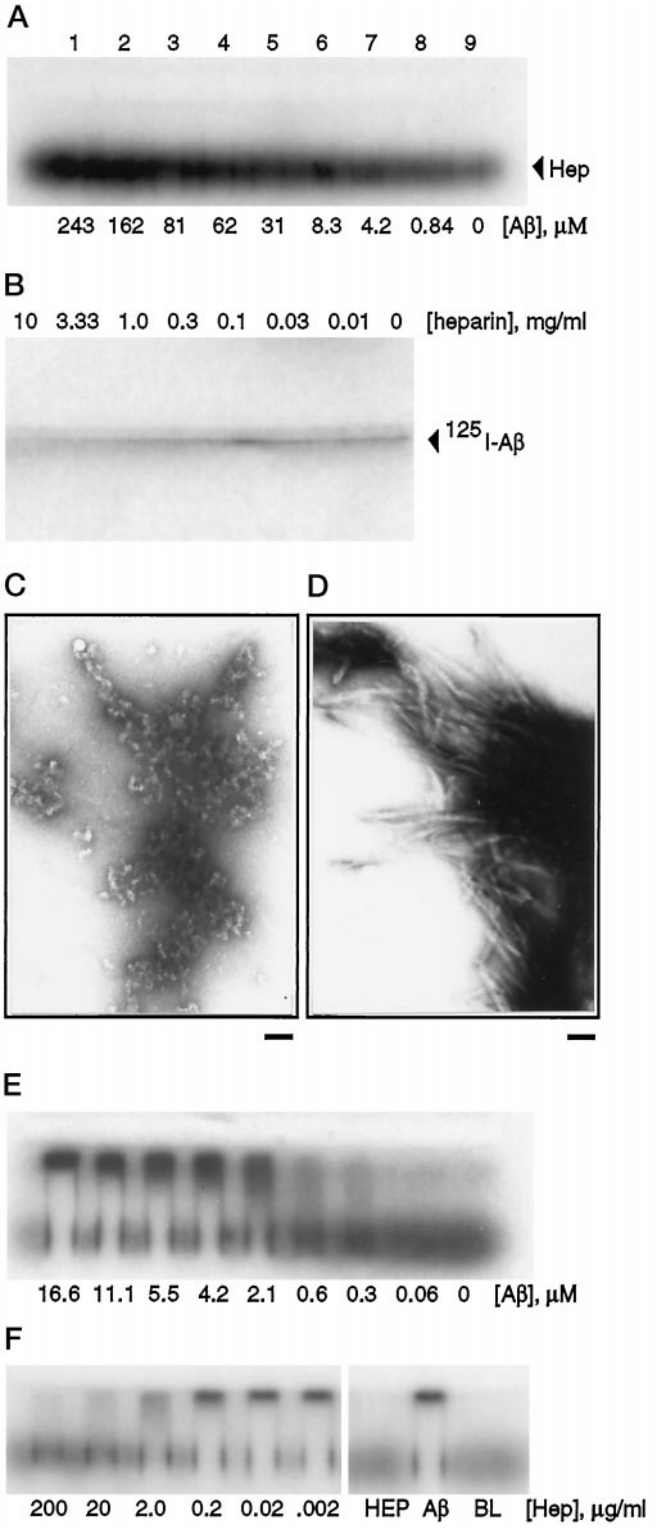

FIG. 2. **Heparin binding profiles of fibrillar and nonfibrillar wild type $A\beta_{1-40}$.** *A*, ACE gel: labeled heparin was electrophoresed through protein wells 1–9 containing the indicated concentrations of unlabeled nonfibrillar Aβ, as determined by amino acid analysis. *B*, reverse ACE gel: increasing concentrations of unlabeled heparin were electrophoresed through a slot of $^{125}I\text{-}A\beta_{1-40}$ (*arrow*). In *A* and *B*, no complex formation is observed. *C*, electron micrograph of the nonfibrillar Aβ preparation. Original magnification, ×80,000. *Bar*, 50 nm. *D*, electron micrograph of the fibrillar Aβ preparation. Original magnification, ×80,000. *Bar*, 50 nm. *E*, ACE gel: protein wells 1–9 contain the indicated concentration of fibrillar Aβ as determined by amino acid analysis. Concentrations as low as 300 nM fibrillar Aβ begin to shift the mobility of heparin, indicating an interaction. *F*, ACE gel: unlabeled LMW-heparin competitively inhibits the binding of ^{125}I-LMW-heparin to fibrillar Aβ. *Lanes 1–6* contain 6.56 μM fibrillar Aβ plus the indicated concentrations of cold LMW-heparin. *Lane 7* (*HEP*) contains 200 μg/ml unlabeled LMW-heparin only; *lane 8* (*Aβ*) contains 6.56 μM fibrillar Aβ only; *lane 9* (*BLANK*) contains ACE electrophoresis buffer only.

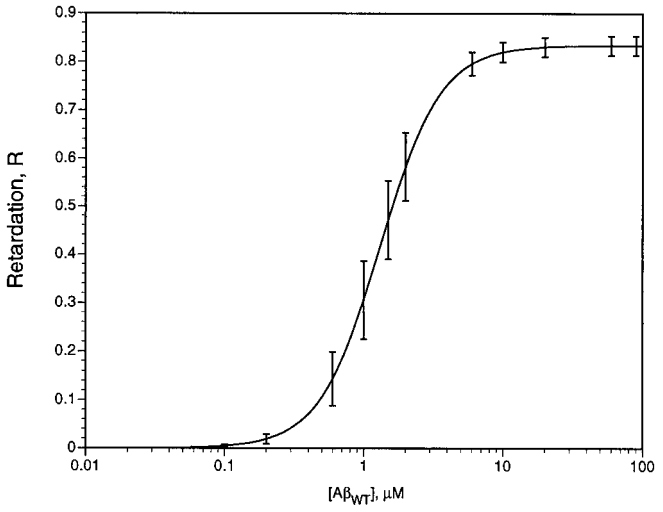

FIG. 3. **Graph of the affinity of heparin for wild type Aβ fibrils as determined by ACE.** Retardation coefficients from ACE gels are graphed as a function of protein concentration. Each set of data ($n = 5$) was fit to the equation $R = R_\infty/(1 + (K_d/[\text{protein}])^2)$ (see "Experimental Procedures"). The mean curve ($K_d = 1.31$ μM) is shown with standard error bars.

peptide concentration (Fig. 5*C*). Values of K_d were calculated as described above, and results from several independent preparations of fibrillar $A\beta_{E22Q}$ yielded an average K_d of 3.45 ± 0.08 μM. This is in the low micromolar range, similar to the value measured for heparin binding to wild type Aβ fibrils prepared by the same method.

In contrast, when Aβ was subjected to a milder aggregation protocol, we observed a distinct difference in the heparin-binding behavior of wild type and mutant peptides. In this case, each peptide was neutralized, incubated for 48 h at 4 °C at a concentration of 1 mM in water and then lyophilized. Immediately after resuspension in water, the wild type Aβ remained in a non-heparin binding state (data not shown). However, after identical treatment, the mutant peptide was able to bind heparin (Fig. 6*A*) and showed an affinity similar to that of preformed $A\beta_{E22Q}$ fibrils. We interpreted this result as indicating that water-aggregated $A\beta_{E22Q}$ adopted a structure similar to that of wild type Aβ that had been aggregated in artificial CSF (*i.e.* fibrils with substantial β-pleated sheet conformation). Further evidence for the presence of this conformation came from the fact that the interaction of heparin with the treated $A\beta_{E22Q}$ was blocked by Congo red in a dose-dependent manner (Fig. 6*B*). In addition, the ability of these $A\beta_{E22Q}$ samples to bind heparin was reversed by overnight incubation in (1,1,1,3,3,3)-hexafluoroisopropanol (HFIP) for 72 h and lyophilization (Fig. 6*C*). HFIP is a solvent that is thought to promote or stabilize α-helices (33), and that can also reverse the neurotoxicity of fibrillar Aβ in cell cultures (34).

The Human Isoform of Amylin Binds Heparin—The presence of heparan sulfate has been demonstrated immunohistochemically in amyloid deposits from most human amyloidotic diseases (for review, see Ref. 16). One well known example is the islet amyloid of type II diabetes (35). In this disease, the 37-residue amyloid subunit protein, called amylin, is the major constituent of the extracellular amyloid deposits that surround pancreatic islet cells. *In vitro*, the human isoform of amylin

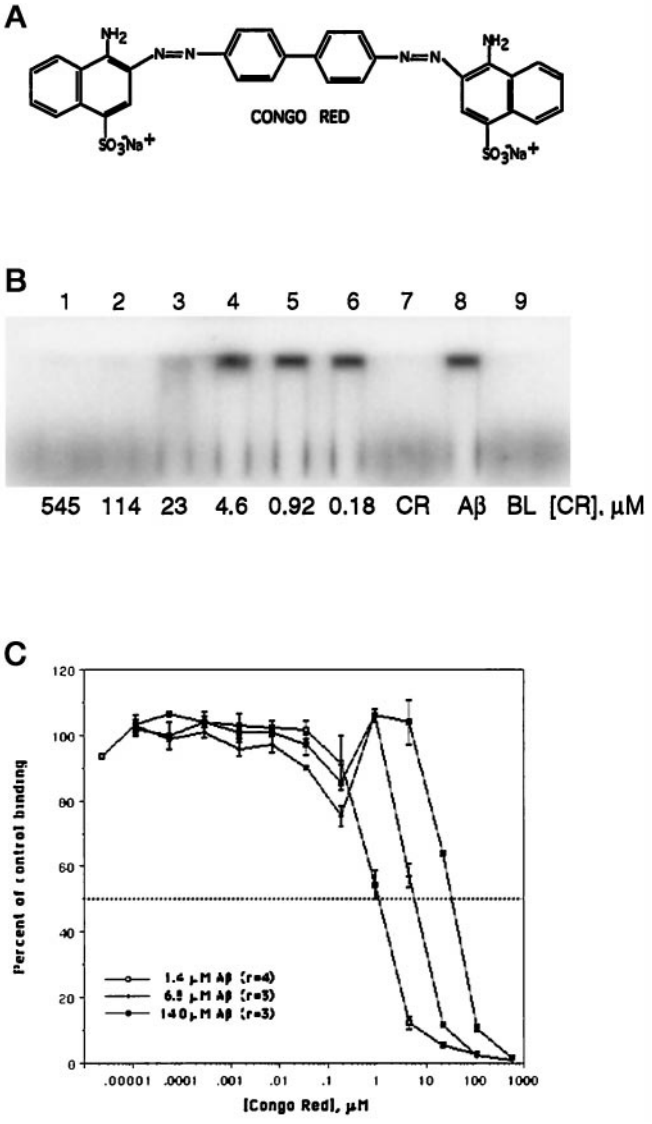

FIG. 4. **Congo red inhibits the binding of Aβ fibrils to heparin.** *A*, ACE gel: *lanes 1–7* contain 6.56 μM Aβ fibrils plus the indicated doses of Congo red. *Lane 7* (*CR*) contains Congo red only; *lane 8* (*Aβ*) contains Aβ fibrils only; *lane 9* (*BL*) contains ACE electrophoresis buffer only (blank). *B*, solution-phase binding assay (see "Results"): comparison of the inhibition curves and IC_{50} for Congo red determined at three concentrations of Aβ.

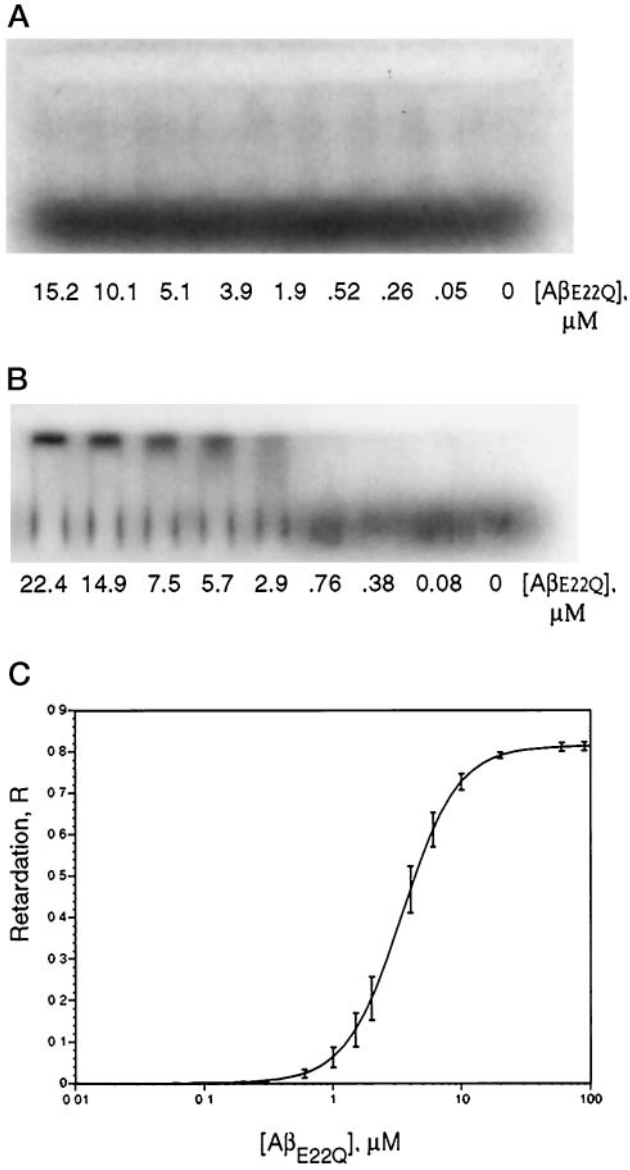

FIG. 5. **Heparin binding profiles of mutant HCHWA-D $Aβ_{E22Q}$.** *A*, ACE gel: protein lanes are loaded with the indicated concentrations of nonfibrillar $Aβ_{E22Q}$. *B*, ACE gel: protein lanes are loaded with the indicated concentrations of fibrillar $Aβ_{E22Q}$. *C*, graph of the affinity of heparin for $Aβ_{E22Q}$ fibrils: each set of data ($n = 5$) was fit to the equation $R = R_\infty/(1 + (K_d/[\text{protein}])^2)$ (see "Experimental Procedures"). The mean curve ($K_d = 3.45$ μM) is shown with standard error bars.

readily forms fibrils that are toxic to cultured islet cells (36). However, the six amino acid substitutions in the rat isoform (Fig. 7*A*) prevent both its assembly into fibrils and its cytotoxicity (36). We used ACE to test the heparin-binding properties of the human and rat isoforms of amylin. Each was freshly resuspended in water from lyophilized aliquots. ACE profiles of ^{125}I-LMW-heparin binding to HPLC-purified human and rat amylin are shown in Fig. 7 (*B* and *C*). Human amylin bound to heparin at peptide concentrations as low as 200 nM, whereas rat amylin did not bind to heparin even at 16.7 μM. Amylin peptides obtained from two different sources (Bachem and Peninsula Laboratories) gave identical results (data not shown). Only the human isoform was birefringent after Congo red staining (not shown), indicating its aggregation and β-pleated conformation. Congo red blocked the amylin-heparin interaction in a dose-dependent manner (Fig. 7*D*), and the heparin-binding structure could be removed by centrifugation at low speed (Fig. 6*E*).

DISCUSSION

Heparan sulfate proteoglycans are integral and invariant components of parenchymal and vascular amyloid deposits in Alzheimer's disease and other amyloidoses. However, characterization of the binding interaction between HSPG and Aβ has been hindered by the unique difficulties of working with Aβ, a 40–42-residue amphipathic peptide that readily precipitates into insoluble aggregates *in vitro*. Since monomers, short oligomers and fibrils of Aβ have different biochemical properties and are likely to have different roles in AD pathology, methods used to study the interaction of Aβ and HSPG should affect as little as possible the aggregation state of the Aβ peptides.

In this paper, we have used ACE in native agarose gels at physiological pH and ionic strength to evaluate heparin-Aβ binding and explore its dependence on Aβ primary and secondary structure.

Examination of the primary amino acid sequence of Aβ re-

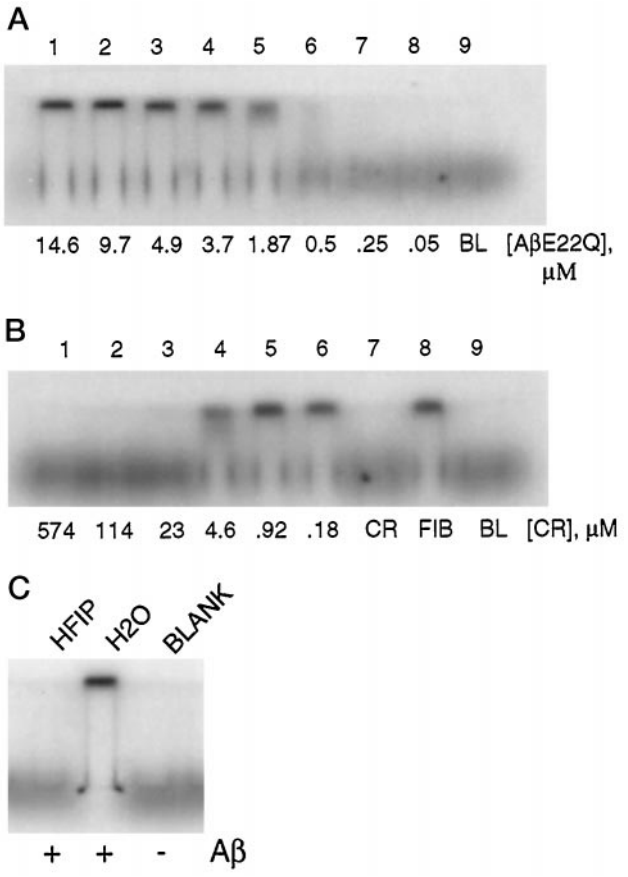

FIG. 6. **Properties of water-aggregated HCHWA-D $A\beta_{E22Q}$.** *A*, ACE gel: the heparin-binding profile of $A\beta_{E22Q}$ following neutralization, incubation in plain water at 4 °C for 48 h, relyophilization, and subsequent resuspension in water. *B*, ACE gel: increasing concentrations of Congo red block the binding of water-aggregated AβE22Q to heparin. *Lanes 1–6* contain 9.7 μM water-aggregated $A\beta_{E22Q}$ plus the indicated dose of Congo red. *Lane 7* (*CR*) contains 574 μM Congo red only; *lane 8* (*FIB*) contains 9.7 μM water-aggregated $A\beta_{E22Q}$ only; *lane 9* (*BL*) contains ACE electrophoresis buffer only (blank). *C*, incubation for 72 h in the α-helix promoting solvent: (1,1,1,3,3,3)-hexafluoroisopropanol reverses the heparin-binding property of water-aggregated $A\beta_{E22Q}$. *Lane 1* (*HFIP*) contains 5.75 μM HFIP-treated $A\beta_{E22Q}$; *lane 2* (*H_2O*) contains 5.85 μM $A\beta_{E22Q}$ alone; *lane 3* (*BLANK*) contains ACE electrophoresis buffer alone.

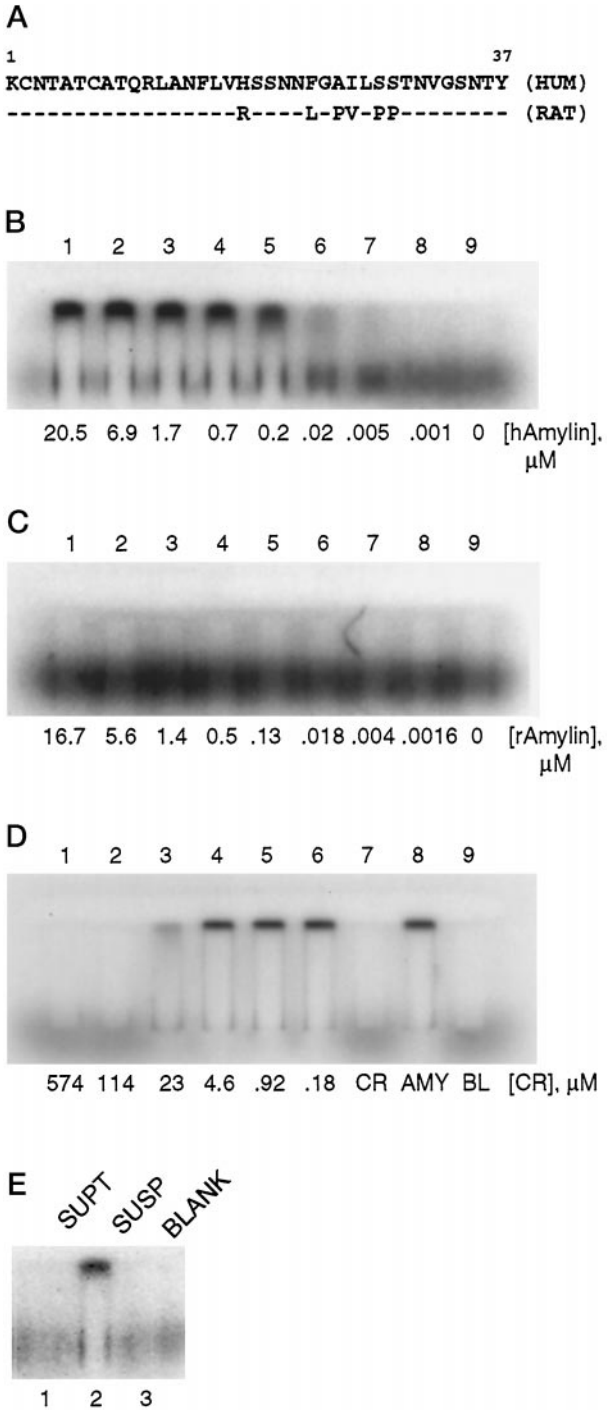

FIG. 7. **Heparin-binding profiles of human and rat amylin on ACE gels.** *A*, amino acid sequences of human and rat amylin. A *dash* indicates identity. *B*, ACE gel: the indicated concentrations of freshly resuspended human amylin were tested for heparin-binding. *C*, freshly resuspended rat amylin does not bind heparin up to concentrations of 16.7 μM. *D*, increasing concentrations of Congo red block the binding of heparin to human amylin. *Lanes 1–6* contain 14.2 μM human amylin plus the indicated dose of Congo red; *lane 7* (*CR*) contains 574 μM Congo red only; *lane 8* (*AMY*) contains 14.2 μM human amylin only; *lane 9* (*BL*) contains ACE electrophoresis buffer only (blank). *E*, centrifugation removes the heparin-binding amylin from solution. *Lane 1* (*SUPT*) contains the supernatant of human amylin (originally 27.3 μM) following centrifugation of the suspension for 15 min at 14,000 rpm; *lane 2* (*SUSP*) contains the uncentrifuged total amylin suspension; *lane 3* (*BLANK*) contains ACE electrophoresis buffer alone.

veals that residues 12–17 (VHHQKL) fit the proposed consensus for a linear heparin-binding site (*X*BB*X*B*X*, where B is a basic residue) (37). However, from our experiments using up to 350 μM nonfibrillar $A\beta_{1-40}$, we conclude that in the structural context of nonfibrillar Aβ, VHHQKL is an inactive heparin-binding sequence. Brunden *et al.* (20) reached a similar conclusion by showing that the corresponding synthetic hexapeptide does not bind to a heparin affinity column at neutral pH.

In contrast to nonfibrillar Aβ, fibrillar Aβ readily bound to heparin. Our measurements, using ACE, show that the affinity of heparin for wild type $A\beta_{1-40}$ fibrils is in the very low micromolar range. Importantly, this value was calculated using the molarity of Aβ monomers, as determined by amino acid analysis; a calculation based on the molarity of fibrils would yield a much lower K_d. The number of monomers per fibril is unknown and is probably highly variable *in vivo*; however, a hypothetical fibril containing 10^4 monomers with a measured K_d of 2 μM would have a K_d of 200 pM when expressed in units of fibril concentration. Our results appear to be consistent with those of Gupta-Bansal *et al.* (38).

We used low molecular weight heparin in our tests of binding to Aβ fibrils to decrease the possibility of multiple Aβ-binding sites along the heparin chain length. Future experiments using defined heparin fragments of progressively lower molecular weight may help to determine the minimum region on a hep-

arin chain required for fibril binding. Additionally, we used fully formed Aβ fibrils to exclude any simultaneous effects of heparin on Aβ aggregation and to measure only the binding affinity of heparin for a characterized population of Aβ. With the recent isolation of stable protofibrillar intermediates in the pathway of Aβ fibrillogenesis (39, 40), it is now possible to compare the heparin-binding properties of Aβ monomers, low molecular weight oligomers, protofibrils, and other intermediates. We favor the hypothesis that endogenous HSPGs (especially their long, sulfated heparan sulfate chains) initially may bind to one or more of these intermediates, creating a template for further Aβ aggregation.

The specific amino acids on the surface of amyloid fibrils that mediate the heparin-Aβ interaction remain to be identified. In the structural context of fibrillar Aβ, the linear VHHQKL epitope within an Aβ monomer might adopt a conformation that enables it to bind heparin. Alternatively, basic residues from multiple Aβ monomers that are brought together on the fibril surface may constitute the heparin-binding site. Examples of proteins in which positively charged heparin-binding "patches" are formed from basic residues contributed by multiple protein domains or subunits include type I collagen and basic fibroblast growth factor (reviewed in Ref. 41).

The marked accumulation of mutant Aβ peptides in the basement membranes of meningeal and cerebral blood vessels in HCHWA-D amyloidosis led us to speculate that this mutant Aβ might have a higher affinity for vascular basement membrane HSPGs. Indeed, the HCHWA-D mutation (Glu → Gln) removes one negative charge from the $A\beta_{1-40}$ peptide, which could theoretically enhance its binding to sulfated HS chains. As measured by ACE, however, the heparin-binding properties of the mutant peptide were similar to those of wild type peptide for both the fibrillar (binding) and nonfibrillar (non-binding) forms. ACE experiments using the mutant $A\beta_{E22Q}$ did demonstrate that the mutant peptide assumed a heparin-binding conformation more readily than the wild type. This finding is consistent with previous studies which showed the enhanced ability of $A\beta_{E22Q}$ to stably self-associate *in vitro* (42–45). Two additional lines of evidence support β-sheet structure as a feature essential for heparin-binding. First, the amyloid-binding dye Congo red blocked the interaction; and second, incubation of $A\beta_{E22Q}$ in the α helix-promoting solvent HFIP reversed its ability to bind heparin.

Amylin is the major protein subunit of pancreatic amyloid deposits in patients with type II diabetes. Lorenzo *et al.* (36) demonstrated that full-length human amylin formed amyloid-like fibrils *in vitro* and was toxic to cultures of pancreatic islet cells. The six amino acid substitutions in the rat isoform of amylin (three of them conservative and three that introduce prolines in place of alanines and serines) blocked both the fibril formation and toxicity of amylin (36). Because HSPGs have been detected immunohistochemically in the pancreatic amyloid deposits of type II diabetes (35), we investigated the binding of amylin to heparin. Despite the lack of a linear consensus heparin-binding sequence (*i.e. X*BB*X*B*X*; Ref. 37), freshly resuspended human amylin from two different sources avidly bound to heparin. In contrast to Aβ, we found that freshly resuspended human amylin bound to heparin immediately. This may be due either to a novel linear heparin-binding epitope or, more probably, due to the strong tendency of human amylin to assume an insoluble β-sheet conformation in water. The ability of Congo red to block the interaction, the removal of the heparin-binding species by brief low speed centrifugation, and the lack of heparin binding by rat amylin all support the latter hypothesis.

In Alzheimer's disease, the pathological consequences of Aβ binding to HSPGs could include protection from proteolytic degradation and clearance (38, 46), and/or creation of a favorable surface for further Aβ deposition. Cell surface proteoglycans may also play a direct role in mediating the neurotoxic effects of Aβ (47). These various observations raise the possibility that pharmacologic inhibition of the HSPG-Aβ interaction could be a means of therapeutic intervention in AD. For example, Congo red is known to block the neurotoxicity of Aβ (47, 48), and we have shown here that Congo red also inhibits Aβ binding to glycosaminoglycans. Congo red analogues that are able to penetrate the blood-brain barrier might ameliorate the neurotoxicity of aggregated Aβ as well as prevent the formation or maturation of new Aβ deposits. As a first step, it would be interesting to determine whether Congo red analogues retard the development of cerebral amyloidosis and subsequent AD neuropathology in a transgenic mouse model of Alzheimer's disease (49, 50). Oral administration of other small sulfated or sulfonated compounds were highly effective in reducing the progression of inflammation-associated AA amyloidosis in an experimental mouse model (51), so this approach seems feasible.

Finally, the major HSPG of adult brain parenchyma is probably glypican (52), a cell-surface HSPG expressed by many populations of neurons. Our preliminary experiments indicate that both glypican and perlecan can bind fibrillar Aβ in ACE assays.[2] In future, we plan to use ACE both to refine the characterization of the heparin-binding conformation of Aβ as well as to more thoroughly characterize the binding of intact HSPGs such as glypican and perlecan to fibrillar and nonfibrillar Aβ.

Acknowledgments—We thank Mary Herndon for helpful comments on the manuscript and Jim Rusche and Dan Witt of Repligen Corporation (Needham, MA) for assistance with the solution-phase binding assay.

REFERENCES

1. Kang, J., Lemaire, H.-G., Unterbeck, A., Salbaum, J. M., Masters, C. L., Greschik, K.-H., Multhaup, G., Beyreuther, K., and Müller-Hill, B. (1987) *Nature* **325,** 733–736
2. Haass, C., Schlossmacher, M. G., Hung, A. Y., Vigo-Pelfrey, C., Mellon, A., Ostaszewski, B. L., Lieberburg, I., Koo, E. H., Schenk, D., Teplow, D. B., and Selkoe, D. J. (1992) *Nature* **359,** 322–325
3. Masters, C. L., Simms, G., Weinman, N. A., Multhaup, G., McDonald, B. L., and Beyreuther, K. (1985) *Proc. Natl. Acad. Sci. U. S. A.* **82,** 4245–4249
4. Selkoe, D. J., Abraham, C. R., Podlisny, M. B., and Duffy, L. K. (1986) *J. Neurochem.* **146,** 1820–1834
5. Roher, A., Wolfe, D., Palutke, M., and KuKuruga, D. (1986) *Proc. Natl. Acad. Sci. U. S. A.* **83,** 2662–2666
6. Abraham, C. R., Selkoe, D. J., and Potter, H. (1988) *Cell* **52,** 487–501
7. Namba, Y., Tomonaga, M., Kawasaki, H., Otomo, E., and Ikeda, K. (1991) *Brain Res.* **541,** 163–166
8. Snow, A. D., Mar, H., Hochlin, D., Kimata, K., Kato, M., Suzuki, S., Hassell, J., and Wight, T. N. (1988) *Am. J. Pathol.* **133,** 456–463
9. Coria, F., Castano, E., Prelli, F., Larrondo-Lillo, M., van Duinen, S., Shelanski, M. L., and Frangione, B. (1988) *Lab. Invest.* **58,** 454–8
10. Eikelenboom, P., and Stam, F. C. (1982) *Acta Neuropathol.* **57,** 239–42
11. Mann, D. M. A., Brown, A., Prinja, D., Davies, C. A., Landon, M., Masters, C. L., and Beyreuther, K. (1989) *Neuropathol. Appl. Neurobiol.* **15,** 317–329
12. Lemere, C. A., Blusztajn, J. K., Yamaguchi, H., Wisniewski, T., Saido, T. C., and Selkoe, D. J. (1996) *Neurobiol. Dis.* **3,** 16–32
13. Snow, A. D., Mar, H., Nochlin, D., Sekiguchi, R. T., Kimata, K., Koike, Y., and Wight, T. N. (1990) *Am. J. Pathol.* **137,** 1253–1270
14. Snow, A. D., Sekiguchi, R. T., Nochlin, D., Kalaria, R. N., and Kimata, K. (1994) *Am. J. Pathol.* **144,** 337–347
15. Joachim, C. L., Morris, J. H., and Selkoe, D. J. (1989) *Am. J. Pathol.* **135,** 309–319
16. Snow, A. D., and Wight, T. N. (1989) *Neurobiol. Aging* **10,** 481–497
17. Yamaguchi, H., Yamazaki, T., Lemere, C. A., Frosch, M. P., and Selkoe, D. J. (1992) *Am. J. Pathol.* **141,** 249–259
18. Luyendijk, W., Bots, G. T. A. M., Vegter-van der Vlis, M., Went, L. N., and Frangione, B. (1988) *J. Neurol. Sci.* **85,** 267–280
19. Levy, E., Carman, M. D., Fernandez-Madrid, I. J., Power, M. D., Lieberburg, I., van Duinen, S. G., Bots, G. T. A. M., Luyendijk, W., and Frangione, B. (1990) *Science* **248,** 1124–1126
20. Brunden, K. R., Richter-Cook, N. J., Chaturvedi, N., and Frederickson, R. C. A. (1993) *J. Neurochem.* **61,** 2147–2154

[2] D. J. Watson, A. D. Lander, and D. J. Selkoe, unpublished data.

21. Buée, L., Ding, W., Delacourte, A., and Fillit, H. (1993) *Brain Res.* **601,** 154–163
22. Buée, L., Ding, W., Anderson, J. P., Narindrasorasak, S., Kisilevsky, R., Boyle, N. J., Robakis, N. K., Delacourte, A., Greenberg, B., and Fillit, H. M. (1993) *Brain Res.* **627,** 199–204
23. Snow, A. D., Kinsella, M. G., Parks, E., Sekiguchi, R. T., Miller, J. D., Kimata, K., and Wight, T. N. (1995) *Arch. Biochem. Biophys.* **320,** 84–95
24. Lee, M. K., and Lander, A. D. (1991) *Proc. Natl. Acad. Sci. U. S. A.* **88,** 2768–2772
25. Herndon, M. E., and Lander, A. D. (1997) in *A Laboratory Guide to Glycoconjugate Analysis* (Jackson, P., and Gallagher, J. T. ed) Birkhauser Verlag AG, Basel, Switzerland, in press
26. Wisniewski, T., Castaño, E., Ghiso, J., and Frangione, B. (1993) *Ann. Neurol.* **34,** 631–33
27. Castaño, E. M., Prelli, F., Wisniewski, T., Golabek, A., Kumar, R. A., Soto, C., and Frangione, B. (1995) *Biochem. J.* **306,** 599–604
28. San Antonio, J. D., Slover, J., Lawler, J., Karnovsky, M. J., and Lander, A. D. (1993) *Biochemistry* **32,** 4746–4755
29. Narang, H. K. (1980) *J. Neuropathol. Exp. Neurol.* **39,** 621–31
30. Merz, P. A., Wisniewski, H. M., Somerville, R. A., Bobin, S. A., Masters, C. L., and Iqbal, K. (1983) *Acta Neuropathol.* **60,** 113–24
31. Lim, W. A., Sauer, R. T., and Lander, A. D. (1991) *Methods Enzymol.* **208,** 196–210
32. Klunk, W. E., Pettegrew, J. W., and Abraham, D. J. (1989) *J. Histochem. Cytochem.* **37,** 1273–1281
33. Barrow, C. J., Yasuda, A., Kenny, P. T. M., and Zagorski, M. (1992) *Mol. Biol.* **225,** 1075–1093
34. Pike, C. J., Burdick, D., Walencewicz, A. J., Glabe, C. G., and Cotman, C. W. (1993) *J. Neurosci.* **13,** 1676–87
35. Young, I. D., Ailles, L., Narindrasorasak, S., Tan, R., and Kisilevsky, R. (1992) *Arch. Pathol. Lab. Med.* **116,** 951–954
36. Lorenzo, A., Razzaboni, B., Weir, G. C., and Yankner, B. A. (1994) *Nature* **368,** 756–760
37. Cardin, A. D., and Weintraub, H. J. (1989) *Arteriosclerosis* **9,** 21–32
38. Gupta-Bansal, R., Frederickson, R. C. A., and Brunden, K. R. (1995) *J. Biol. Chem.* **270,** 18666–18671
39. Harper, J. D., Wong, S. S., Lieber, C. M., and Lansbury, P. T. (1997) *Chem. Biol.* **4,** 119–125
40. Walsh, D. M., Lomakin, A., Benedek, G. B., Condron, M. M., and Teplow, D. B. (1997) *J. Biol. Chem.* **272,** 22364–22372
41. Lander, A. D. (1994) *Chem. Biol.* **1,** 73–78
42. Wisniewski, T., Ghiso, J., and Frangione, B. (1991) *Biochem. Biophys. Res. Commun.* **179,** 1247–1254
43. Fraser, P. E., Nguyen, J. T., Inouye, H., Surewicz, W. K., Selkoe, D. J., Podlisny, M. B., and Kirschner, D. A. (1992) *Biochemistry* **31,** 10716–10723
44. Clements, A., Walsh, D. M., Williams, C. H., and Allsop, D. (1993) *Neurosci. Lett.* **161,** 17–20
45. Fabian, H., Szendrei, G. I., Mantsch, H. H., and Otvos Jr, L. (1993) *Biochem. Biophys. Res. Commun.* **191,** 232–239
46. Snow, A. D., Sekiguchi, R., D, N., Fraser, P., Kimata, K., Mizutani, A., Arai, M., Schreier, W. A., and Morgan, D. G. (1994) *Neuron* **12,** 219–234
47. Shaffer, L. M., Dority, M. D., Gupta-Bansal, R., Frederickson, R. C., Younkin, S. G., and Brunden, K. R. (1995) *Neurobiol. Aging* **16,** 737–45
48. Yan, G. M., Lin, S. Z., Du, Y., Fuson, K., May, P. C., Irwin, R. P., and Paul, S. M. (1996) *Neurobiol. Aging* **17,** S109 (abstr.)
49. Games, D., Adams, D., Alessandrini, R., Barbour, R., Berthelette, P., Blackwell, C., Carr, T., Clemens, J., Donaldson, T., Gillespie, F., Guido, T., Hagopian, S., Johnson-Wood, K., Khan, K., Lee, M., Leibowitz, P., Lieberburg, I., Little, S., Masliah, E., McConlogue, L., Montoya-Zavala, M., Mucke, L., Paganini, L., Penniman, E., Power, M., Schenk, D., Seubert, P., Snyder, B., Soriano, F., Tan, H., Vitale, J., Wadsworth, S., Wolozin, B., and Zhao, J. (1995) *Nat. Med.* **373,** 523–527
50. Hsiao, K., Chapman, P., Nilsen, S., Eckman, C., Harigaya, Y., Younkin, S., Yang, F., and Cole, G. (1996) *Science* **274,** 99–102
51. Kisilevsky, R., Lemieux, L. J., Fraser, P. E., Kong, X., Hultin, P. G., and Szarek, W. A. (1995) *Nat. Med.* **1,** 143–148
52. Lander, A. D., Stipp, C. S., and Ivins, J. K. (1996) *Perspect. Dev. Neurobiol.* **3,** 347–359